THE LIVERMORE HIGH INTENSITY ELECTRON STORAGE RING

J. W. Beal, R. K. Cooper, W. A. Lamb, V. K. Neil and L. Smith

University of California, Lawrence Livermore Laboratory, Livermore, California, USA.

Abstract

A high intensity electron storage ring is being constructed at Lawrence Livermore Laboratory. The purpose of this device is the study of the effects of electromagnetic self-forces at beam currents up to 1000 A and energies up to 6 MeV. In the initial stage of operation no RF cavity will be used. A lifetime of at least a few ms is contemplated, and the design is such that at peak current the negative mass and resistive wall instabilities are expected to occur within this time. The effect of various inductive structures on longitudinal stability will be investigated. Experimental studies will be made to elucidate the phenomena associated with transverse beam stability. The ring has a circumference of 28.8 m. The aluminum vacuum tank has a circular cross section of 2 ft in diameter. Air core magnets provide the magnetic fields of the eight-section FDO lattice. The quadrupole doublet and the zero gradient bending magnets are separately powered, but superimposed in space. To facilitate study of resonance effects, Q-values between 1.5 and 2.5 are obtainable.

1. Introduction

An electron storage ring is under construction at Lawrence Livermore Laboratory. The design value for the circulating current in the ring is 1000 A, with the electrons being provided by the Astron linear induction accelerator. With this device various known(and probably some unknown) beam instabilities will be studied with a view toward their elimination. The Astron accelerator presently provides 500 to 800 A of electrons at 6 MeV with a pulse duration of 0.3 μs. Although the energy varies by a few percent over the length of the pulse, the instantaneous energy spread in the beam is of the order of 0.1%. The emittance of the accelerator is typically 50π mrad/cm.

The phenomena associated with intense beams have been extensively studied by accelerator theorists for several years. However, experimental confirmation of most of the predicted effects has either never been accomplished, or at best, these effects have been observed at an intensity level two or three orders of magnitude below the levels contemplated in the storage ring. Moreover, most of the problems encountered in present storage rings were not anticipated theoretically. The parameters of the storage ring were chosen with some flexibility so that known harmful effects may be either avoided, or observed and possibly controlled.

2. Description of the Ring

The over-all size of the storage ring was dictated in part by the space available. The total circumference is 28.8 m, consisting of eight straight sections and eight 45° bending sections. All sections are 1.8 m in length. The vacuum tank, which is constructed on one-inch thick aluminum, has a circular minor cross section of radius 30 cm. Single turn injection will be accomplished with a fast pulsed arrangement of conductors inside the vacuum tank that provides the transverse magnetic field required to place particles on the desired orbit. The injection system places a lower limit on the length of a straight section.

The bending and focusing fields are provided by two layers of air-core magnet windings placed on the outside of each curved section. The inner layer provides the zero-gradient bending field. The outer layer consists of two coils, each extending over one half of the curved section, and providing respectively the focusing and defocusing quadrupole fields. The design of these magnets is described in Ref. 1. The three sets of bending magnets, focusing quadrupoles, and defocusing quadrupoles are each powered in series, with separate trimming provided for each magnet. The lattice is such that both the radial and vertical tunes may be varied from 1.5 to 2.5. A parameter list is given in Table I for operation at 5 MeV and for $Q_x = Q_y = 1.75$.

3. Beam Dynamics Studies

The parameters of the ring were chosen on the basis of simple existing theory of several known effects to be investigated. In particular, it was desired to separate the growth of instabilities with the hope of studying them one by one.

3.1 Space Charge Effects

The tune shift arising from the coherent self forces may be expressed in terms of the quantity Q_1 defined by the relation

$$Q_i^2 = Q_e^2 - Q_1^2 \qquad (1)$$

in which Q_e embodies the focusing forces of the external guide field and Q_i is the total single particle (incoherent) tune. If the beam is centered in a round pipe, there are no forces arising from charges and current in the wall, and for an unneutralized beam we have

$$Q_1^2 = 2nr_e\bar{R}^2/\gamma(\gamma^2 - 1)a^2 \qquad (2)$$

in which n is the number of particles per unit length in the beam, $\bar{R} = (28.8/2\pi)$m, r_e is the classical electron radius, a is the beam radius, and $\gamma(=12)$ is the particle energy in units of m_oc^2. For a = 5 cm and a current of 1000 A we find $Q_1^2 = 0.577$. A strong focusing guide field was chosen to provide a value of Q_e such that the effect of self forces will be significant but not dominant.

Table I Storage Ring Parameters

Design kinetic energy	T	5 MeV
Intensity	I	10^3 A
Guide field at design energy	B_o	79.9 G
Magnetic radius	ρ	2.29 m
Average radius	$\bar{R}$	4.58 m
Circumference	$2\pi\bar{R}$	28.8 m
Number of cells		8
Structure of cell		FDO
Length of cell		3.6 m
Revolution frequency		10.4 MHz
Aperture (radial and vertical)		30 cm
Number of betatron oscillations per revolution		
radial = vertical	$Q_{x,y}$	1.75
Betatron phase advance per cell	μ	78.8°
Betatron wavelength	λ	16.5 m
Betatron amplitude function β		
maximum	β_{max}	4.737 m
minimum	β_{min}	1.672 m
Momentum compaction X_p		
maximum	X_{pmax}	2.032 m
minimum	X_{pmin}	1.344 m
Transition Gamma	γ_{tr}	1.651
Guide field magnets		
number		8
effective length	L_G	1.8 m
field strength	B_o	79.9 G
Quadrupole magnets		
number		16
effective length	L_Q	0.9 m
Profile parameter B'/B_o		
focusing quadrupole	k_f	2.02 m^{-1}
defocusing quadrupole	k_d	-2.46 m^{-1}

The transverse motion of the beam as a whole is affected by the image charges and currents in the surrounding wall. These forces may be expressed in terms of the quantity Q_2, which is defined by the relation

$$Q_c^2 = Q_e^2 - Q_2^2 \tag{3}$$

in which Q_2 embodies the image forces and Q_c is the total coherent tune. If the electric and magnetic images coincide, we have

$$Q_2^2 = 2nr_e\bar{R}^2/\gamma(\gamma^2 - 1)b^2 \tag{4}$$

in which b is the minor radius of the vacuum tank. The finite conductivity of the wall causes the magnetic images to decay with time. After the magnetic images have decayed completely, we have

$$Q_2^2 = 2nr_e\bar{R}^2/\gamma\beta^2b^2 \tag{5}$$

The decay of the magnetic images may result in unstable coherent transverse motion of the beam if Q_c passes through an integer value during the decay. This effect is described in detail in Ref. 2. For the parameters of the storage ring, the growth of this unstable motion is sufficiently slow that it will not interfere with observations of the much faster transverse resistive wall instability. If desired, the insertion of liners in the vacuum tank would allow a study of the effects of image current decay.

3.2 Effect of Residual Gas

Provided that the background gas is ionized only by scattering of the beam particles, the ion density increases linearly with time and raises the incoherent tune. For example, with $Q_e = 1.75$ and a background pressure of 10^{-7} torr, the total incoherent tune reaches a value of 2 in 400 μs. The vacuum system will provide a base pressure of 10^{-9} torr, thus allowing investigation of the effects of background gas over a range of pressure.

3.3 Negative Mass Instability

Investigation and suppression of the negative mass instability is necessary in order to study other instabilities that are less well understood. The growth time of the negative mass instability in the absence of frequency spread is given by

$$\tau_g = \frac{Q_x\gamma}{\omega_o}\left(\frac{\gamma}{nr_e g}\right)^{1/2} \tag{6}$$

in which Q_x is the radial tune, and ω_o the particles' angular circulation frequency. For the storage ring $g = 1 + 2\ell n(b/a)$. For $Q_x = 1.75$, and again for a current of 1000 A, we find $\tau_g = 2.1$ μs. It should be noted that Eq. (6) yields the growth time for the fundamental mode (i.e., one wavelength around the machine). For a mode with ℓ wavelengths around the machine τ_g is inversely proportional to ℓ. The energy spread necessary for stability is 2.5%. By varying the current and perhaps the energy spread, one can investigate the existing theory of this instability. Various methods utilizing inductive walls will be employed in an attempt to suppress the instability. Although well founded in theory, to date there has been little if any experimental evidence of the success of these methods.

3.4 Transverse Resistive Wall Instability

For coherent oscillation of the beam in the axial direction the growth rate of the resistive wall instability is given by

$$\tau_g = \frac{Q_z \gamma}{2nr_e}\left(\frac{b}{R}\right)^3 \frac{(8\pi\sigma\omega)^{\frac{1}{2}}}{\omega_o^2} \qquad (7)$$

in which b is the minor radius of the vacuum tank (30 cm), and σ is the conductivity of the wall material (2×10^{17} sec^{-1}, typical of aluminum). The frequency $\omega = (\ell - Q_z)\omega_o$, with ℓ an integer. For $Q_z = 1.75$ and for $\ell = 2$ we calculate τ_g and find $\tau_g = 130$ μs. This time is sufficiently longer than the growth time for the negative mass instability to enable independent study. Of particular interest is an investigation of the stabilizing effect of a spread in the quantity $(\ell - Q_z)\omega_o$. The instability has been successfully suppressed by feedback and there is little or no experimental evidence for stabilization by Landau damping.

A schematic drawing of the ring is shown in Fig. 1. The major components of the ring are being assembled, as shown in Fig. 2, and it is hoped that experiments will begin in the near future.

References

1. R.K. Cooper, J.W. Beal and V.K. Neil, "A Method for the Design of Air Core Magnets in Toroidal Geometry," LRL Document UCRL-73203 Preprint, March 1971; to be published in Particle Accelerators.

2. S. Bodner, V.K. Neil and L. Smith, Particle Accelerators 1, 327 (1970).

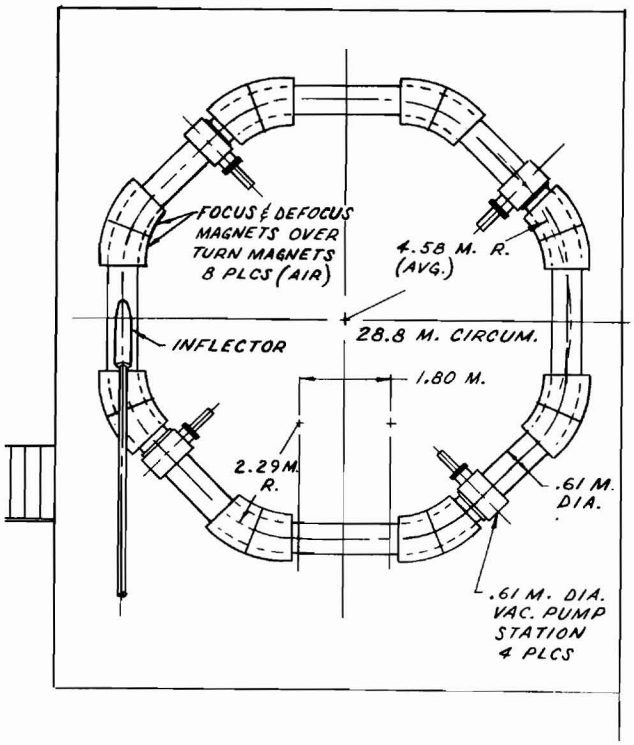

Fig. 1. Schematic Drawing of Ring

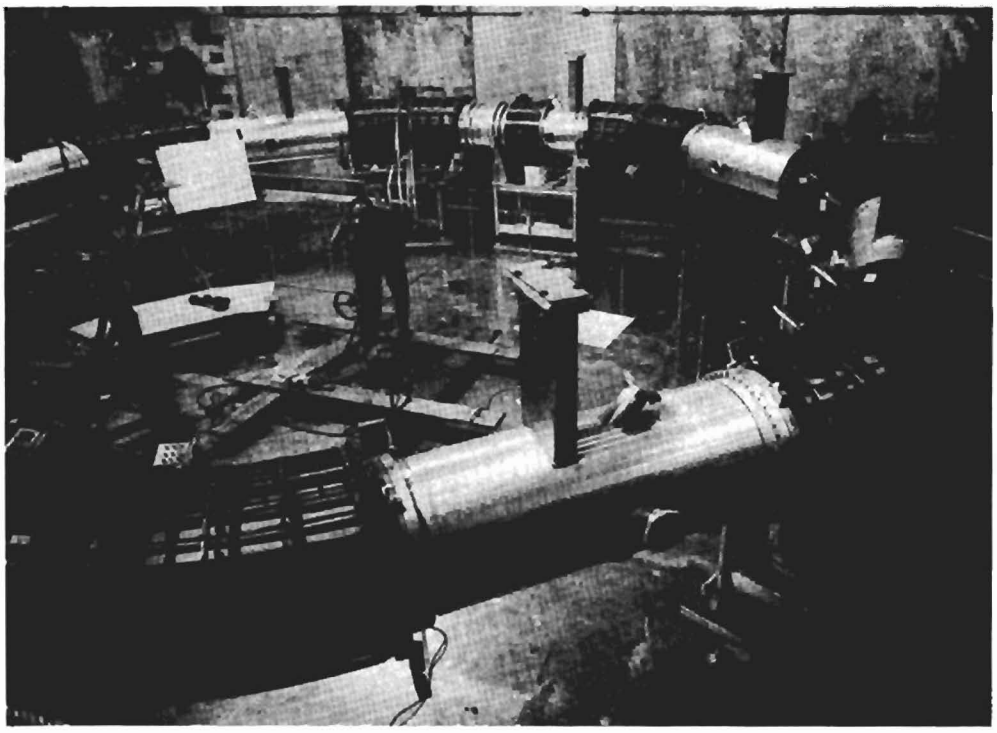

Fig. 2. Components of Ring Being Assembled